Changes of Low-Frequency Vibrational Modes Induced by Universal ^{15}N- and ^{13}C-Isotope Labeling in S_2/S_1 FTIR Difference Spectrum of Oxygen-Evolving Complex†

Yukihiro Kimura,*,‡ Naoki Mizusawa,‡ Asako Ishii,‡ Toshihiro Yamanari,§ and Taka-aki Ono*,‡

Laboratory for Photo-Biology (1), RIKEN Photodynamics Research Center, Institute of Physical and Chemical Research, 519-1399 Aoba, Aramaki, Aoba, Sendai 980-0845, Japan, and Faculty of Integrated Arts and Sciences, Hiroshima University, 1-7-1 Kagamiyama, Higashi-Hiroshima 739-8521, Japan

Received August 8, 2003; Revised Manuscript Received September 21, 2003

ABSTRACT: The effects of universal ^{15}N- and ^{13}C-isotope labeling on the low- (650−350 cm^{-1}) and mid-frequency (1800−1200 cm^{-1}) S_2/S_1 Fourier transform infrared (FTIR) difference spectrum of the photosynthetic oxygen-evolving complex (OEC) were investigated in histidine-tagged photosystem (PS) II core particles from *Synechocystis* sp. PCC 6803. In the mid-frequency region, the amide II modes were predominantly affected by ^{15}N-labeling, whereas, in addition to the amide II, the amide I and carboxylate modes were markedly affected by ^{13}C-labeling. In the low-frequency region, by comparing a light-induced spectrum in the presence of ferricyanide as the electron acceptor, with the double difference S_2/S_1 spectrum obtained by subtracting the Q_A^-/Q_A from the $S_2Q_A^-/S_1Q_A$ spectrum, considerable numbers of bands found in the light-induced spectrum were assigned to the S_2/S_1 vibrational modes in the unlabeled PS II core particles. Upon ^{13}C-labeling, changes were observed for most of the prominent bands in the S_2/S_1 spectrum. Although ^{15}N-labeling also induced changes similar to those by ^{13}C-labeling, the bands at 616(−), 605(+), 561(+), 555(−), and 544(−) cm^{-1} were scarcely affected by ^{15}N-labeling. These results indicated that most of the vibrational modes found in the low-frequency spectrum are derived from the coupling between the Mn-cluster and groups containing nitrogen and/or carbon atom(s) in a direct manner and/or through hydrogen bonding. Interestingly, an intensive band at 577(−) cm^{-1} was not affected by ^{15}N- and ^{13}C-isotope labeling, indicating that this band arises from the mode that does not include either nitrogen or carbon atoms, such as the skeletal vibration of the Mn-cluster or stretching vibrational modes of the Mn-ligand.

Photosynthetic oxygen evolution takes place in the oxygen-evolving complex (OEC),[1] in which the catalytic center is comprised of a tetranuclear Mn-cluster located in the lumenal side of the photosystem (PS) II. Two water molecules are oxidized through a light-driven oxidation cycle via five intermediate states, which are labeled as S_n ($n = 0-4$). Among the S-states, S_0 and S_4 are the most reduced and the most unstable intermediate states, respectively. S_n advances to S_{n+1} by absorbing each photon and reaches the S_4 state after cumulative accumulation of four oxidizing equivalents. The S_4 state spontaneously relaxes to the S_0 state concomitant with the release of an oxygen molecule (*1*−*4*). It has been shown that both Ca^{2+} and Cl^- ions are indispensable inorganic cofactors for the oxygen evolution (*1*, *5*). In a stepwise manner, the Mn-cluster is oxidized upon the advancement of each step of the S-state cycling and reduced upon the $S_3-(S_4)-S_0$ transition; however, the S_2 to S_3 transition may not be accompanied by the direct oxidation of the cluster. X-ray crystallographic analysis of the PS II complex from *Thermosynechococcus elongatus* at 3.8 Å by Zouni et al. (*6*) has suggested that the electron density of the Mn-cluster fits the trimer−monomer-like structure; however, the individual Mn-ions were not resolved in the electron density map. This situation has not improved in subsequent reports (*7*, *8*); neither the coordination structure of the Mn-cluster nor the information concerning the amino acid residues of the putative ligands for the Mn-cluster were provided. Nevertheless, potential candidates for the ligands for the Mn-cluster have been proposed based on the results of site-directed mutagenesis studies; amino acid residues of the D1 protein including Asp-170, His-190, His-332, Glu-333, His-337, Asp-342, and Ala-344 are possible ligands of the Mn-cluster (*9*). In addition, extensive studies employing various techniques including EPR spectroscopy (*10*, *11*) and X-ray absorption spectroscopy (*12*, *13*) have provided

† This research was supported by grants for the Frontier Research System and Special Postdoctoral Researchers Program at RIKEN and Grant-in-Aid for Young Scientists (B) (14780518) (Y.K.) from MEXT of Japan.

* To whom correspondence should be addressed. Tel: +81 (22) 228 2047. Fax: +81 (22) 228 2045. E-mail: (Y.K.) ykimura@postman.riken.go.jp; (T.-a.O.) takaaki@postman.riken.go.jp

‡ RIKEN.

§ Hiroshima University.

[1] Abbreviations: OEC, oxygen-evolving complex; PS, photosystem; Chl, chlorophyll; Q_A, primary quinone acceptor of photosystem II; Q_B, secondary quinone acceptor of photosystem II; Y_Z, redox active tyrosine of the D1 protein; FTIR, Fourier transform infrared; EPR, electron paramagnetic resonance; DCMU, 3-(3, 4-dichlorophenyl)-1,1-dimethylurea; MES, 2-morpholinoethanesulfonic acid; PCR, polymerase chain reaction; kb, kilobase pairs.

10.1021/bi035420q CCC: $25.00
Published on Web 10/24/2003

detailed information on the magnetic and structural properties of the Mn-cluster and its coordination sphere. However, our knowledge of the OEC is still insufficient for resolving the mechanism of the oxygen evolution.

To understand the mechanism, details of the chemical structure and the reaction of the OEC would be required. Fourier transform infrared (FTIR) spectroscopy is a highly promising method for probing these properties. Accordingly, it has been extensively applied in the mid-frequency region (4000−1000 cm^{-1}) for studying the structural changes of protein matrixes and potential amino acid ligands for the Mn-cluster (*14*−*36*), as well as water molecules interacting with the OEC (*23*, *32*, *35*) during the S-state cycling. Furthermore, more direct information on the chemical nature of the Mn-ligands and Mn-substrates can be provided using the low-frequency region of the IR spectrum. In contrast to those in the mid-frequency region, the application of FTIR to the OEC in the low-frequency region has been rather limited due to technical difficulties. Light-induced FTIR spectrum for S_2/S_1 in the low-frequency region (1000−350 cm^{-1}) has been reported, and some important information that cannot be accessed by mid-frequency measurements was obtained (*20*, *24*, *25*, *28*, *31*). The results indicated that, based on the downshifts of the bands upon ^{18}O-water substitution (*24*), the bands at 606(+) and 625(−) cm^{-1} are attributed to the Mn−O−Mn cluster mode in the S_2- and S_1-states. Furthermore, this cluster mode was affected by the replacement of Ca^{2+}- with Sr^{2+}-ions, suggesting that the mode is associated with Ca^{2+}-ions through a network of hydrogen bonds (*24*). The shift of the Mn−O−Mn cluster mode at 606(+) cm^{-1} to 612(+) cm^{-1} in the D1-Asp170His mutant of *Synechocystis* sp. PCC 6803 with no appreciable difference in the corresponding mid-frequency S_2/S_1 difference spectra suggested structural coupling of Asp170 with the Mn-cluster (*28*). However, the obtained spectrum was obscured by interferences due to intense bands of ferricyanide (413 and 389 cm^{-1}) and ferrocyanide (592 cm^{-1}), which were included as an electron acceptor (ferricyanide) and formed by illumination (ferrocyanide) (*25*).

The reported low-frequency S_2/S_1 spectrum (*24*) revealed numerous bands that were not affected by ^{18}O-water substitution, and some of these bands may include the modes reflecting Mn-ligand interactions. The assignments of these bands are, therefore, crucial to understand the spectrum. In the present study using light-induced FTIR difference spectroscopy, upon the light-induced oxidation of the Mn-cluster from S_1- to S_2-states, changes were detected in the low-frequency (650−350 cm^{-1}) vibrational modes of the PS II core particles of *Synechocystis* sp. PCC 6803. Effects on the low-frequency vibrational modes due to the universal ^{15}N- and ^{13}C-isotope labeling of the core particles were examined, and the observed isotopic bands were analyzed. Possible assignments of the major bands in the low-frequency S_2/S_1 spectrum are discussed based on these findings.

MATERIALS AND METHODS

Construction of Synechocystis Strain Containing His-Tagged CP47. The genomic DNA was prepared from *Synechocystis* sp. strain PCC 6803 as described in the literature (*37*) and amplified by PCR using a specific primer set corresponding to 1506 bp *psbB* and 641 bp downstream flanking DNA. The amplified DNA was cloned and sequenced, followed by the insertion of six histidine codons, $(CAC)_6$, before the TAG stop codon of *psbB* using a commercial oligonucleotide-mediated mutagenesis kit (LA PCR in vitro Mutagenesis Kit, Takara). The resulting recombinant plasmid was cloned and sequenced. Finally, the 0.3 kb *Nco*I/*Nco*I fragment containing a part of the unidentified open region frame, *slr0907*, was replaced by a 1.5 kb fragment of the plasmid pTER34 (a generous gift from Dr. M. Ikeuchi, University of Tokyo) conferring resistance to erythromycin (Er^r). All constructed DNAs were cloned into pUC19 and maintained in the *E. coli* DH5-α strain. The final plasmid, pN47His, was transformed into the cells of the *Synechocystis* host strain, in which a 0.9 kb *Sma*I/*Nco*I fragment of *psbB*, containing the stop codon of *psbB* and the part of *slr0907*, was replaced by a 1.3 kb fragment of the plasmid pUC4K (Amersham Pharmacia Biotech) conferring resistance to kanamycin (Km^r). A putative transformant was selected for its ability of photoautotrophic growth in the presence of erythromycin (1 μg/mL). After segregation, the genomic DNA was isolated, and the PCR-amplified *psbB* gene was sequenced. The resulting transformant, N47His, was maintained on solid BG 11 media containing erythromycin (1 μg/mL).

Culture Conditions. The transformed *Synechocystis* cells were photoheterotrophically grown in BG-11 medium supplemented with 5 mM glucose at 30 °C under 30−50 μmol photons/m^2/s in an 8 L Clearboy (NALGENE). For global ^{15}N-labeling, the culture was grown using 10 mM $Na^{15}NO_3$ (99.5% ^{15}N-enrichment, Shoko Tsusho) as the sole nitrogen source during cell growth and bubbled with 2% CO_2-enriched air. The final Chl concentration of the cells was 10 μg/mL. For global ^{13}C-labeling, the culture was grown using 4 mM glucose-U-^{13}C (98.3% ^{13}C-enrichment, Shoko Tsusho) as the sole carbon source and gently bubbled with pure air that was free of CO and CO_2 (<1 ppm CO and CO_2, Nippon Sanso).

Preparation of Synechocystis PS II Core Particles. Cyanobacteria cells harvested by centrifugation at 4700*g* were suspended in a small volume of medium A (10 mM $MgCl_2$, 5 mM $CaCl_2$, 25% (w/v) glycerol, and 50 mM Mes/NaOH, pH 6.0) and then stored in liquid N_2. The following procedures were performed under darkness or dim green light at 0−4 °C unless otherwise noted. Cells were disrupted with Bead-Beater (Bio-Spec Products) as described (*38*) with modifications. After thawing, the cells in medium A were disrupted using glass beads (diameter of 0.105−0.125 mm) in a Bead-Beater chamber, using 17 cycles of a break sequence (10 s of homogenization followed by 2.5 min of cooling). After dilution with medium A, the homogenate was centrifuged at 39 900*g* for 15 min. The precipitate was resuspended in medium A at 1 mg of Chl/mL and then solubilized using 0.8% (w/v) *n*-dodecyl-β-D-maltoside (GLYCON Biochemicals) for 20 min with gentle stirring. After the precipitation of unsolubilized cells by centrifugation at 39 900*g* for 15 min, the resulting supernatant was loaded on a Ni-NTA column (Qiagen), which was preequilibrated with medium A supplemented with 0.04% *n*-dodecyl-β-D-maltoside. After the column was washed with 3−4 bed volumes of the same buffer, the PS II core particles were eluted with medium A supplemented with 50 mM histidine and 0.04% dodecyl maltoside. The eluent was precipitated using centrifugation at 39 900*g* for 10 min in the presence

of PEG 6000 (10%, w/v) and then resuspended in medium A and stored in liquid N_2. The oxygen-evolution activity of the obtained His-tagged PS II core particles was approximately 2500 μmol of O_2 (mg of Chl)$^{-1}$ h^{-1} at 25 °C with potassium ferricyanide as an electron acceptor. For FTIR measurements, the PS II core particles were washed three times with medium B (400 mM sucrose, 20 mM NaCl, 20 mM $CaCl_2$, and 20 mM Mes/NaOH, pH 6.0) in the presence of 10% (w/v) PEG 6000, followed by extensive washes using medium B.

Sample Preparations for FTIR Measurements. The PS II core particles from *Synechocystis* were suspended in medium B in the presence of 2 mM sodium ferricyanide as an electron acceptor to obtain the single-pulse-induced spectrum. Alternatively, the sample suspension contained 0.1 mM DCMU for the $S_2Q_A^-/S_1Q_A$ spectrum or 0.1 mM DCMU and 10 mM NH_2OH for the Q_A^-/Q_A spectrum. NH_2OH and DCMU were added as an electron donor and as an inhibitor of the electron transfer from Q_A to Q_B. The sample suspension was centrifuged at 176 000*g* for 10 min, and the resulting pellet was sandwiched between a pair of AgCl disks. The spectra were measured under conditions that provided the absorbance of the sample of less than 1.0, at 1657 cm^{-1} for measuring spectra in 1800−1200 cm^{-1} region and at 650 cm^{-1} for measuring spectra in the 650−350 cm^{-1} region.

FTIR Measurements. Mid-frequency (1800−1200 cm^{-1}) FTIR spectra were recorded on a Bruker IFS-66v/s spectrophotometer equipped with an MCT detector (EG&G Optoelectronics D316/6). A custom-made CdTe band-pass filter (>25% transmission in the 2000−350 cm^{-1} range) was placed in front of the sample to block the He−Ne laser beam leaking from the interferometer compartment and to improve the signal-to-noise ratio. Low-frequency (650−350 cm^{-1}) FTIR spectra were recorded on a Bomen MB102 spectrophotometer equipped with a Si bolometer (Infrared, HDL-5). CdTe filters were placed in front of the sample to block the He−Ne calibration beam and at the back of the sample to protect the detector element from laser scattering. Sample temperature was maintained at 250 K using a homemade cryostat and temperature controller (Chino, KP1000). Samples were illuminated using one of two methods: by CW-light (HOYA-SCHOTT HL150R) passing through a long-pass filter (≥620 nm) for the $S_2Q_A^-/S_1Q_A$ and Q_A^-/Q_A difference spectra or by a single pulse from a frequency-doubled Nd^{3+}:YAG laser (Spectra Physics INDI-50, 532 nm, pulse width 6−7 ns) for the single-pulse-induced S_2/S_1 difference spectrum. Single-beam spectra were collected at 4 cm^{-1} resolution over 70 s in the mid-frequency (150 scans) and in the low-frequency (60 scans) regions. Light-induced difference spectra were obtained by subtracting the single-beam spectrum acquired before the flash from that after the flash. To improve the signal-to-noise ratio, 20−26 difference spectra for the mid-frequency region and 45−69 difference spectra for low-frequency region were obtained and averaged.

RESULTS AND DISCUSSION

Effects of ^{15}N- and ^{13}C-Labeling on the Mid-Frequency S_2/S_1 Spectra. The differences between the mid-frequency S_2/S_1 difference spectra of the unlabeled (Figure 1A, red line) and ^{15}N-labeled (Figure 1A, blue line) PS II core particles from the *Synechocystis* sp. PCC 6803 are shown as the

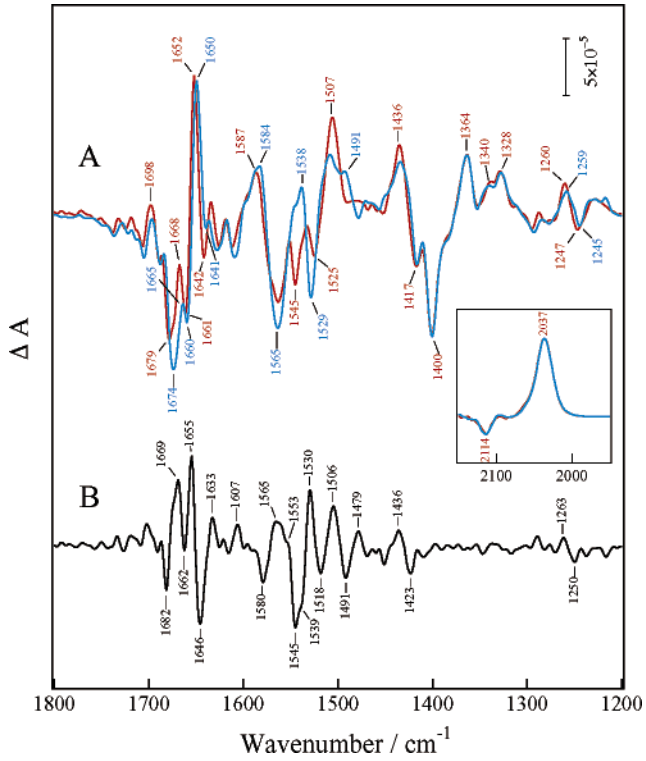

FIGURE 1: Mid-frequency S_2/S_1 difference spectra of unlabeled (A, red line) and ^{15}N-labeled (A, blue line) PS II core particles from *Synechocystis* sp. PCC 6803. Samples were illuminated with a single pulse from a frequency-doubled Nd^{3+}:YAG laser (532 nm, 6−7 ns, 10 mJ/cm^2/pulse) at 250 K. Sample suspension included 2 mM ferricyanide as an exogenous electron acceptor. Double difference ^{14}N/^{15}N spectrum (B) was obtained by subtracting the ^{15}N-labeled S_2/S_1 from the unlabeled S_2/S_1 spectrum after normalization with respect to the CN stretching bands of ferricyanide (2114 cm^{-1}) and ferrocyanide (2037 cm^{-1}), as shown in the inset. See text for details.

double difference ^{14}N/^{15}N spectrum (Figure 1B). The double difference spectrum was obtained by subtracting the ^{15}N-labeled spectrum from the unlabeled one after normalization with respect to the peak-to-peak intensity at the bands for the CN stretching modes of ferrocyanide/ferricyanide (2037(+)/2114(−) cm^{-1}), which changed stoichiometrically due to the light-induced reduction of ferricyanide to ferrocyanide (Figure 1, inset). Characteristic S_2/S_1 bands were observed in the unlabeled spectra where the symmetric (1450−1300 cm^{-1}) and asymmetric (1600−1500 cm^{-1}) carboxylate stretching modes appeared in addition to the prominent amide I (1700−1600 cm^{-1}) and amide II (1600−1500 cm^{-1}) modes (*14*, *20*, *29*). Upon ^{15}N-labeling, several bands shifted to lower frequencies, especially in the amide II regions where the CN stretching and NH bending modes of the polypeptide backbone appear. The double difference ^{14}N/^{15}N spectrum clearly showed that the bands at 1580(−), 1553(+), 1545(−), and 1506(+) cm^{-1} shifted to lower frequencies by 14−15 cm^{-1} to 1565(+), 1539(−), 1530(+), and 1491(−) cm^{-1}, respectively. These bands were assigned to the amide II modes since the ^{15}N-labeling dependent downshift is consistent with that of the amide II band in the absorption spectra (data not shown). Smaller downshifts of 1−5 cm^{-1} detected in the amide I region (1700−1600 cm^{-1}) were in agreement with those of the amide I modes of polypeptides, which are mostly assigned to the CO stretching mode with minimal contributions from the NH bending mode. Although the symmetric (1450−1300 cm^{-1}) and asymmetric (1600−1500

cm^{-1}) carboxylate stretching bands were basically unaffected by the ^{15}N-labeling, the absence of shifts in the latter region was uncertain due to the overlap of the prominent amide II mode.

The observed effects of ^{15}N-labeling on the spectrum were consistent with those previously reported for spinach (*14*) and *T. elongatus* (*36*). However, there are several differences: the 1652(+) cm^{-1} band that has been reported to increase significantly (*36*) showed only a minor change in intensity with a downshift of 2 cm^{-1}. Second, the band at 1436(+) that has been reported to show no isotopic changes (*36*) was observed to downshift by 13 cm^{-1} to 1423(−), suggesting that the vibrational modes from nitrogen-containing groups may partly contribute to this mode. Third, small but distinct isotopic bands with a shift of 13 cm^{-1} were found at 1263(+)/1250(−) cm^{-1} in the double difference spectrum. It was previously proposed that the bands at 1260−1255 cm^{-1} included the COH bending modes of Tyr at 1255 cm^{-1} (*16*, *26*) and/or Ser or Thr at 1260 cm^{-1} (*36*). Moreover, it has been reported that ^{15}N-labeling did not cause any shifts of these bands (*36*). However, the present result indicated that these bands involved either the mode of an amino acid side chain containing a nitrogen atom or the amide III mode, which is mostly comprised of C−N stretching and N−H in-plane bending modes. Some of the differences between the present and the previously reported results may be in part attributable to the difference in sample materials and/or conditions of the spectra measurements.

The mid-frequency S_2/S_1 difference spectra of unlabeled (Figure 2A, red line) and ^{13}C-labeled (Figure 2A, green line) PS II core particles from *Synechocystis* were used to calculate the double difference $^{12}C/^{13}C$ spectrum (Figure 2B). In contrast to the ^{15}N-labeling (Figure 1), considerable changes were observed, not only in the amide regions but also in the carboxylate regions by ^{13}C-labeling. In the amide I region (Figure 2A), the bands at 1707(−), 1698(+), 1679(−), 1661(−), 1652(+), 1642(−), and 1635(+) cm^{-1} downshifted by 40−50 cm^{-1} to 1662(−), 1651(+), 1631(−), 1620(−), 1610(+), 1601(−), and 1593(+) cm^{-1}, respectively. Since these downshifts were consistent with the shifts of the amide I peak position in the absorption spectrum of the PS II cores upon ^{13}C-labeling (data not shown), these bands can be assigned to the CO stretching of the polypeptide backbone. Furthermore, ^{13}C-labeling caused bands at 1552(+), 1545(−), and 1507(+) cm^{-1} to downshift by 12−20 cm^{-1} to 1539(+), 1525(−), and 1495(+) cm^{-1}. These bands were assigned to the amide II modes, including the NH bending mode coupled to the CN stretching mode since the downshift of the amide II peak in the absorption spectrum of the PS II cores upon ^{13}C-labeling was 14 cm^{-1} (data not shown). These results are generally consistent with those previously reported for *T. elongatus* (*22*, *36*). The bands at 1587(+), 1565(−), and 1507(+) cm^{-1} (Figure 2A), which were unaffected by ^{15}N-labeling, downshifted to 1556(+), 1525(−), and 1466(+) cm^{-1}, respectively, upon ^{13}C-labeling and thus allowed the assignment of these bands to the asymmetric COO^- stretching modes of the carboxylate group. Accordingly, the symmetric carboxylate stretching modes at 1436(+), 1417(−), 1400(−), and 1364(+) cm^{-1} were downshifted by 25−35 cm^{-1} to 1404(+), 1385(−), 1375(−), and 1333(+) cm^{-1}, respectively. Since the positive band at 1436 cm^{-1} was shifted by ^{15}N-labeling, and also presumably by ^{13}C-labeling, it can be suggested that this band corresponds to a moiety involving nitrogen and/or carbon atoms.

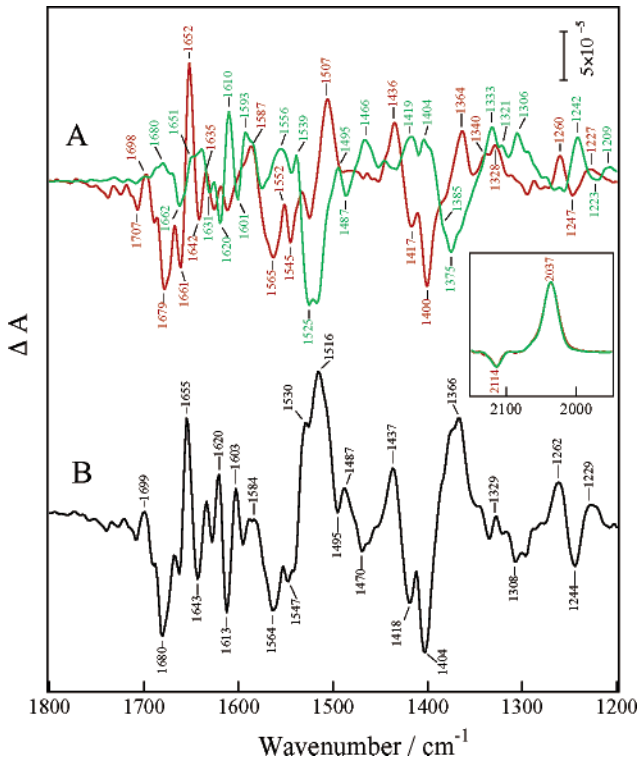

FIGURE 2: Mid-frequency S_2/S_1 difference spectra of unlabeled (A, red line) and ^{13}C-labeled (A, green line) PS II core particles from *Synechocystis* sp. PCC 6803. Samples were illuminated at 250 K with a single pulse in the presence of 2 mM ferricyanide. The double difference $^{12}C/^{13}C$ spectrum (B) was obtained by subtracting the ^{13}C-labeled S_2/S_1 from the unlabeled S_2/S_1 spectrum after normalization with respect to the CN stretching bands of ferricyanide (2114 cm^{-1}) and ferrocyanide (2037 cm^{-1}), as shown in the inset. See text and legend of Figure 1 for details.

The bands at 1340(+) and 1328(+) cm^{-1} also seemed to downshift by 19−22 cm^{-1} to 1321(+) and 1306(+) cm^{-1}, respectively. It has been reported that the L-[1-^{13}C]alanine-labeling of *Synechocystis* can induce isotopic shifts in the putative carboxylate modes of the C-terminal Ala-344 at ~1600 cm^{-1} and in the 1360−1300 cm^{-1} region in the S_2/S_1 spectrum (*30*). The observed isotopic bands in those regions may, therefore, correspond to the symmetric and asymmetric carboxylate stretching modes of the C-terminal Ala-344 of the D1 protein. In addition, upon the ^{13}C-labeling, the differential band at 1260(+)/1247(−) cm^{-1} in the unlabeled S_2/S_1 spectrum was downshifted to 1242(+)/1223(−) cm^{-1}, which is consistent with the suggestion that this differential band involves a COH mode of Tyr, Ser, or Thr (*16*, *26*, *36*). Tyrosine and alanine, however, may not contribute to the positive band at 1260 cm^{-1} since neither ring-4-^{13}C-tyrosine labeling (*16*) nor l-[1-^{13}C] alanine labeling (*30*) affected this band. It is important to note that the intensity of the $^{12}C/^{13}C$ isotopic bands at 1262(+)/1244(−) cm^{-1} was significantly greater than that of the $^{14}N/^{15}N$ bands at 1263(+)/1250(−) cm^{-1} (see Figure 1B). This difference suggests minor contributions from the amide III mode (CN stretching mode coupled to the NH bending mode) in this region since both isotopic bands in the amide III modes were expected to be affected equally. Possible contributions of the non-heme iron and/or Q_A at the acceptor side of the PS II to the observed S_2/S_1 spectra are negligible since neither

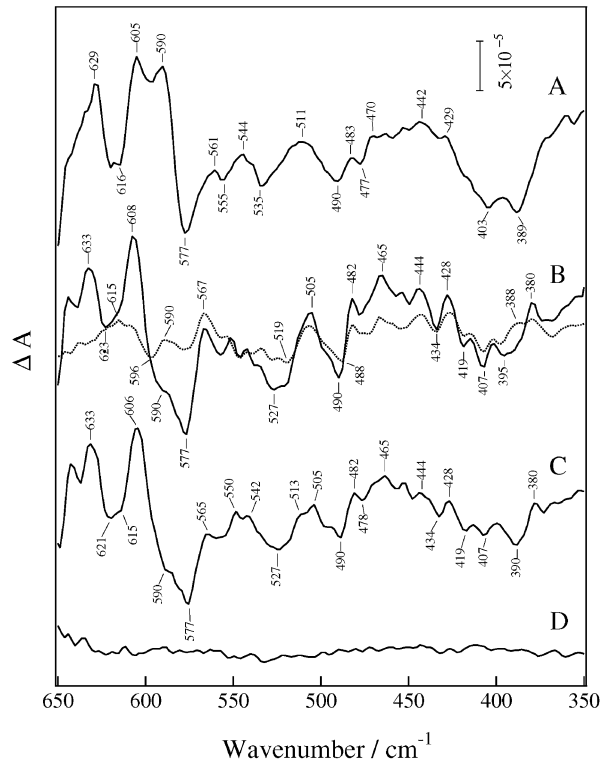

FIGURE 3: Low-frequency vibrational modes in the light-induced spectrum of unlabeled PS II core particles from *Synechocystis* sp. PCC 6803. Unlabeled PS II core particles were illuminated at 250 K in the presence of 2 mM ferricyanide as an exogenous electron acceptor (A), in the presence of 0.1 mM DCMU with no electron acceptor for the $S_2Q_A^-/S_1Q_A$ difference spectrum (B, solid line), and in the presence of 0.1 mM DCMU and 10 mM NH_2OH for the Q_A^-/Q_A difference spectrum (B, broken line). Samples were illuminated with a single pulse from a frequency-doubled Nd^{3+}:YAG laser (532 nm, 6−7 ns, 10 mJ/cm^2/pulse) (A) or with CW-light (2 mW/cm^2) (B). The Q_A^-/Q_A difference spectrum was presented after normalization as described in the text. The double difference S_2/S_1 spectrum (C) was obtained by subtracting the Q_A^-/Q_A difference from the $S_2Q_A^-/S_1Q_A$ difference spectrum. A dark-minus-dark spectrum (D) was presented to show the noise level. See text for details.

the ring CN stretching mode of the histidine ligands for the non-heme iron nor the prominent CO stretching mode of Q_A^- was detected in the mid-frequency S_2/S_1 spectra. This indicates that light illumination under the present experimental conditions induced insignificant redox changes on the acceptor side of PS II.

Low-Frequency S_2/S_1 Spectra. The low-frequency (650−350 cm^{-1}) light-induced difference spectra of the unlabeled PS II core particles from *Synechocystis* are shown in Figure 3. As shown in the single-pulse induced light-minus-dark spectrum in the presence of ferricyanide as the electron acceptor (Figure 3A), prominent bands were observed at 629-(+), 616(−), 605(+), 590(+), 577(−), 403(−), and 389(−) cm^{-1} in addition to the medium intensity bands at 561(+), 555(−), 544(+), 535(−), 511(+), 490(−), 483(+), 477(−), 470(+), 442(+), and 429(+) cm^{-1}. Major characteristics of the spectrum were similar to those previously reported by Chu et al. for spinach (*24*, *25*, *31*) and *Synechocystis* (*28*); however, the present spectrum showed improved resolution of more bands due to the higher number of accumulations. The spectrum consisted mainly of the S_2/S_1 and ferrocyanide/ferricyanide difference spectra, and little of the bands associated with the reduction of non-heme iron and/or Q_A at the acceptor side, as clearly demonstrated by the absence of these bands in the mid-frequency spectra measured under identical experimental conditions (Figure 1A and unpublished data). The negative band at ∼400 cm^{-1} can be assigned as Fe−C stretching or FeCN bending mode of ferricyanide, whereas the positive band at ∼590 cm^{-1} can be assigned to the Fe−C stretching mode of ferrocyanide generated by the light-induced reduction of the ferricyanide (*25*, *39*). To obtain the S_2/S_1 spectrum that is free from the ferrocyanide/ferricyanide modes, the $S_2Q_A^-/S_1Q_A$ and Q_A^-/Q_A difference spectra were determined using unlabeled PS II core particles.

The light-induced $S_2Q_A^-/S_1Q_A$ (solid line) and Q_A^-/Q_A (broken line) difference spectra of unlabeled PS II core particles from *Synechocystis* are shown in Figure 3B. For the measurements of the $S_2Q_A^-/S_1Q_A$ and Q_A^-/Q_A spectra, DCMU was included as an inhibitor of the electron transfer from Q_A to Q_B, whereas, for the Q_A^-/Q_A spectrum, NH_2OH was included as an exogenous electron donor. Under the present experimental conditions, these adventitious chemicals did not exhibit any bands in the 650−350 cm^{-1} region. Except for the absence of the bands at 590(+) and around 400(−) cm^{-1} (mainly due to ferrocyanide and ferricyanide), the spectral features of the $S_2Q_A^-/S_1Q_A$ spectrum were roughly comparable to those of the light-induced spectrum in the presence of ferricyanide (Figure 3A), implying that the band intensities of the Q_A^-/Q_A spectrum are smaller than those of the S_2/S_1 spectrum. The Q_A^-/Q_A difference spectrum featured bands at 615(+), 596(−), 590(+), 567(+), 519(−), 505(+), 488(−), 482(+), 465(+), 444(+), 428(+), 419-(−), 407(−), 388(+), and 380(+) cm^{-1}. It is of note that, based on the mid-frequency spectra measured under identical conditions (data not shown), the $S_2Q_A^-/S_1Q_A$ and Q_A^-/Q_A spectra did not include any bands from the non-heme iron. The double difference S_2/S_1 spectrum (Figure 3C) was calculated by subtracting the Q_A^-/Q_A difference spectrum (Figure 3B, broken line) from the $S_2Q_A^-/S_1Q_A$ difference spectrum (Figure 3B, solid line) so as to minimize the difference between the double difference spectrum (Figure 3C) and the single-pulse-induced spectrum (Figure 3A) in the frequency region where bands for ferricyanide and ferrocyanide were not expected to exist. This is due to the absence of an appropriate band that can be used for normalizing the $S_2Q_A^-/S_1Q_A$ and Q_A^-/Q_A spectra for the subtraction. Except for the ferrocyanide/ferricyanide bands, the band positions and overall features of the obtained spectrum were consistent with those of the single-pulse-induced spectrum. The obtained double difference S_2/S_1 spectrum may, therefore, be a somewhat accurate representation of the actual low-frequency S_2/S_1 spectrum. However, some of the artifacts induced by the subtraction cannot be completely ignored due to the relatively low S/N ratio of the low-frequency spectra and/or some possible alterations of the Q_A^-/Q_A spectrum between the Mn-depleted and oxygen-evolving PS II. Notably, the obtained S_2/S_1 spectrum exhibited only a faint negative shoulder at ∼590 cm^{-1} in the region for ferrocyanide but showed several bands at ∼400 cm^{-1} in the region for ferricyanide.

Effects of ^{15}N- and ^{13}C-Labeling on the Low-Frequency S_2/S_1 Spectra. The double difference $^{14}N/^{15}N$ spectrum (Figure 4B) of the PS II core particles from *Synechocystis* in the presence of ferricyanide was calculated by subtracting the single-pulse-induced spectrum of the universally ^{15}N-

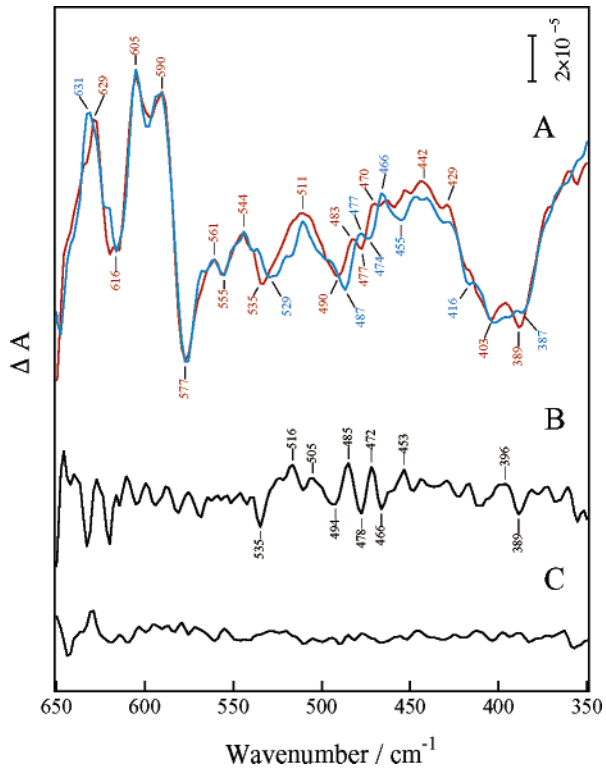

FIGURE 4: Low-frequency S_2/S_1 difference spectra of the unlabeled (A, red line) and ^{15}N-labeled (A, blue line) PS II core particles from *Synechocystis* sp. PCC 6803. Samples were illuminated at 250 K with a single pulse in the presence of 2 mM ferricyanide. The double difference $^{14}N/^{15}N$ spectrum (B) was obtained by subtracting the ^{15}N-labeled S_2/S_1 from the unlabeled S_2/S_1 spectrum after normalization as described in the text. A dark-minus-dark spectrum (C) was presented to show the noise level. The unlabeled spectrum (A, red line) is a reproduction of spectrum in Figure 3A. See text and the legend of Figure 3 for details.

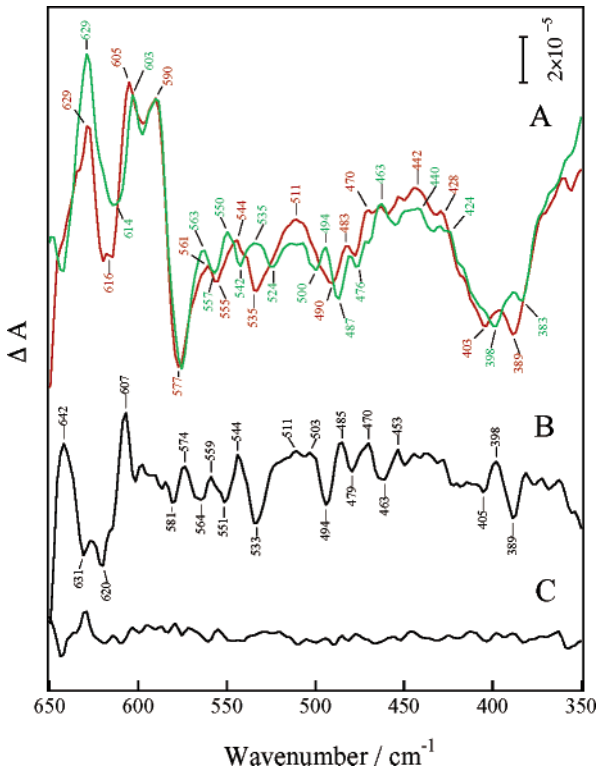

FIGURE 5: Low-frequency S_2/S_1 difference spectra of the unlabeled (A, red line) and ^{13}C-labeled (A, green line) PS II core particles from *Synechocystis* sp. PCC 6803. Samples were illuminated at 250 K with a single pulse in the presence of 2 mM ferricyanide. The double difference $^{12}C/^{13}C$ spectrum (B) was obtained by subtracting the ^{13}C-labeled S_2/S_1 from the unlabeled S_2/S_1 spectrum after normalization as described in the text. A dark-minus-dark spectrum (C) was presented to show the noise level. The unlabeled spectrum (A, red line) is a reproduction of spectrum in Figure 3A. See text and legend of Figure 3 for details.

labeled (Figure 4A, blue line) from the unlabeled spectrum (Figure 4A, red line). Before the subtraction, the spectra were normalized with respect to the peak-to-peak intensity of the bands at 590(+)/577(−) cm^{-1} since the ferrocyanide band at 590 cm^{-1} should not be affected by isotope labeling, and the 577(−) cm^{-1} band was found to be insensitive to either ^{15}N- or ^{13}C-labeling. Upon ^{15}N-labeling, several bands in the range of 540−450 and ∼390 cm^{-1} were downshifted, suggesting that these bands correspond to the coupling between the Mn-cluster and the ligands containing nitrogen atoms. Shifts were also observed for the ∼630 cm^{-1} band, which may be corresponding to the amide IV modes (O═C−N bending and CC stretching modes) of the polypeptide backbone (*40*) or to the ring torsion modes of the histidine residues (*41*). However, large absorption bands due to water molecules in the sample pellet prevented the unequivocal analysis of this region. Vibrational modes at 616(−), 605-(+), 577(−), 561(+), 555(−), and 544(+) cm^{-1} were unaffected by ^{15}N-isotope labeling, suggesting that these bands correspond to vibrational modes that are independent of nitrogen atoms. It is noteworthy that contributions from the non-heme iron on the acceptor side to the isotopic bands were negligible since non-heme iron bands were not detected in the mid-frequency spectrum. In fact, low-frequency vibrational modes that resulted from the light-induced reduction of the non-heme iron (data not shown) were scarcely detected in the spectrum.

The double difference $^{12}C/^{13}C$ spectrum (Figure 5B) of the PS II core particles from *Synechocystis* in the presence of ferricyanide was calculated by subtracting the single-pulse-induced spectra of the universally ^{13}C-labeled (Figure 5A, green line) from the unlabeled (Figure 5A, red line) spectra. The spectra were normalized with respect to the peak-to-peak intensity of the 590(+)/577(−) cm^{-1} bands. Upon ^{13}C-labeling, isotopic bands were observed in the frequency of 640−600 cm^{-1} region, whereas ^{15}N-labeling induced minor changes in the spectrum. Furthermore, the 616(−) and 605-(+) cm^{-1} band peaks were downshifted by 2 cm^{-1}, indicating that these bands correspond to the vibrational modes of carbon-containing groups. Although these bands cannot be unequivocally assigned, possible assignments include the Mn−COO^- bending modes of the putative carboxylate ligands (*20*) or the amide VI mode that mainly involves the C═O out of plane bending mode (*40*), which appears at 600 cm^{-1}. The 606(+) cm^{-1} band has been reported to downshift in ^{18}O-water, and based on the analysis of the band shift, the bands at 606(+) and 625(−) cm^{-1} were assigned to the Mn−O−Mn cluster mode in the S_2- and S_1-states, respectively (*24*). It is conceivable that both the modes derived from the carbon-containing group and the Mn−O−Mn mode are cumulatively induced in this region. Since an upshift of 6 cm^{-1} has been reported for the 606(+) cm^{-1} band in the D1-Asp170His mutant of *Synechocystis* (*28*), it is possible that D1-Asp170 is responsible for the observed effect on the

605(+) cm^{-1} band by ^{13}C-labeling. Upon ^{13}C-labeling, the upshift of the bands at 561(+), 555(−), and 544(+) cm^{-1}, which were not affected by ^{15}N-labeling, suggested that these bands correspond to carbon-containing but not nitrogen-containing group(s).

The medium intensity isotopic bands observed in the 540−370 cm^{-1} region in the $^{12}C/^{13}C$ spectrum (Figure 5B) were comparable to those found in the $^{14}N/^{15}N$ spectrum (Figure 4B). Since amide modes are not likely to appear in this frequency region (*40*), the results suggest that the bands correspond to some amino acid residues containing nitrogen atom(s) in the side chain that are coupled to the Mn-cluster as a direct ligand and/or in an indirect manner through hydrogen bonding. Pulsed EPR (*42*) and mid-frequency FTIR (*21*) studies have suggested that a histidine residue is bound to the Mn-cluster as a direct ligand. It is therefore possible that modes for the imidazole ring of the putative histidine ligand are responsible for the $^{14}N/^{15}N$ and $^{12}C/^{13}C$ isotopic bands. It has been reported that Fe-histidine modes in hemoproteins (*43*, *44*) and Mg-histidine modes in bacterial reaction centers (*45*) appeared at frequencies lower than 250 cm^{-1}. Although these frequencies are considerably lower than those for the observed isotopic bands in the 540−370 cm^{-1}, it is possible that Mn-histidine modes may appear at higher frequencies if the force constants for Mn-histidine modes in the OEC are relatively large. Recent FTIR studies for a tetranuclear manganese adamantan-like complex indicated that several weak bands, induced upon the change in an oxidation state of the complex, in the range of 510−425 cm^{-1} may contain Mn−O modes and suggested that the character of the ligands to the Mn-cluster influences the Mn−O bond strengths and consequently the vibrational modes (*46*). Therefore, it may be also possible that the low-frequency S_2/S_1 bands affected upon ^{15}N- and/or ^{13}C-labeling originated from the Mn-cluster modes that are sensitive to the isotopic exchange of ligands for the cluster. In contrast to the bands affected by ^{15}N- and/or ^{13}C-isotope labeling, the intense negative band at 577 cm^{-1} was hardly affected by the isotopes. Although small isotopic bands were overlapped at 574(+)/581(−) cm^{-1}, as shown in the $^{12}C/^{13}C$ difference spectrum, the results indicate that the major portion of the 577(−) cm^{-1} band is attributable to groups that contain neither nitrogen nor carbon atoms. It has been reported that the negative band at 578 cm^{-1} in the S_2/S_1 spectrum was not affected by the ^{18}O-water exchange (*24*). It is of note in this context that the low-frequency resonance Raman spectra of OEC indicated the presence of the oxo-bridged $Mn_2(\mu\text{-}O)_2$ core modes that were insensitive to the D_2O/H_2O exchange at 587 and 511 cm^{-1} in the S_1-state (*47*). Furthermore, the recent low-frequency Raman spectra and normal coordinate analyses of oxo-bridged manganese model complexes showed that the peak at 566 cm^{-1} is mainly assigned to the symmetric $Mn^{III}-O$ stretching mode of the $Mn_2(\mu\text{-}O)$ core (*48*), supporting the assignment of the 566 cm^{-1} band to the $Mn^{III}-O-Mn^{III}$ stretching vibration (*49*). Therefore, we may consider that the 577(−) cm^{-1} mode corresponds possibly to the ^{18}O-water insensitive skeletal vibration of the Mn-cluster or to the stretching vibrational modes between the Mn-cluster and the oxygen ligand that is not exchangeable with ^{18}O-water.

ACKNOWLEDGMENT

We are thankful to Dr. M. Ikeuchi (University of Tokyo, Japan) for the generous gift of *Synechocystis* sp. PCC 6803 and Dr. Y. Kashino (Himeji Institute of Technology, Japan) for helpful advice on the preparation of the PS II core particles.

REFERENCES

1. Debus, R. J. (1992) *Biochim. Biophys. Acta 1102*, 269−352.
2. Witt, H. T. (1996) *Ber. Bunsen-Ges. Phys. Chem. 100*, 1923−1942.
3. Hoganson, C. W., and Babcock, G. T. (2000) *Met. Ions Biol. Syst. 37*, 613−656.
4. Renger, G. (2001) *Biochim. Biophys. Acta 1503*, 210−228.
5. Yocum, C. F. (1991) *Biochim. Biophys. Acta 1059*, 1−15.
6. Zouni, A., Witt, H.-T., Kern, J., Fromme, P., Krauss, N., Saenger, W., and Orth, P. (2001) *Nature 409*, 739−743.
7. Fromme, P., Kern, J., Loll, B., Biesiadka, J., Saenger, W., Witt, H. T., Krauss, N., and Zouni, A. (2002) *Philos. Trans. R. Soc. London Ser. B 357*, 1337−1345.
8. Kamiya, N., and Shen, J.-R. (2003) *Proc. Natl. Acad. Sci. U.S.A. 100*, 98−103.
9. Debus, R. J. (2001) *Biochim. Biophys. Acta 1503*, 164−186.
10. Geijer, P., Peterson, S., Åhrling, K. A., Deák, Z., and Styring, S. (2001) *Biochim. Biophys. Acta 1503*, 83−95.
11. Peloquin, J. M., and Britt, R. D. (2001) *Biochim. Biophys. Acta 1503*, 96−111.
12. Robblee, J. H., Cinco, R. M., and Yachandra, V. K. (2001) *Biochim. Biophys. Acta 1503*, 7−23.
13. Yachandra, V. K. (2002) *Philos. Trans. R. Soc. London Ser. B 357*, 1347−1358
14. Noguchi, T., Ono, T.-A., and Inoue, Y. (1995) *Biochim. Biophys. Acta 1228*, 189−200.
15. Zhang, H., Razeghifard, M. R., Fischer, G., and Wydrzynski, T. (1997) *Biochemistry 36*, 11762−11768.
16. Noguchi, T., Inoue, Y., and Tang, X.-S. (1997) *Biochemistry 36*, 14705−14711.
17. Hienerwadel, R., Boussac, A., Breton, J., Diner, B. A., and Berthomieu, C. (1997) *Biochemistry 36*, 14712−14723.
18. Zhang, H., Fischer, G., and Wydrzynski, T. (1998) *Biochemistry 37*, 5511−5517.
19. Berthomieu, C., Hienerwadel, R., Boussac, A., Breton, J., and Diner, B. A. (1998) *Biochemistry 37*, 10547−10554.
20. Chu, H.-A., Gardner, M. T., O'Brien, J. P., and Babcock, G. T. (1999) *Biochemistry 38*, 4533−4541.
21. Noguchi, T., Inoue, Y., and Tang, X.-S. (1999) *Biochemistry 38*, 10187−10195.
22. Noguchi, T., Sugiura, M., and Inoue, Y. (1999) in *Fourier Transform Spectroscopy* (Itoh, K., and Tasumi, M. Eds.) pp 459−460, Waseda University Press, Tokyo, Japan.
23. Noguchi, T., and Sugiura, M. (2000) *Biochemistry 39*, 10943−10949.
24. Chu, H.-A., Sackett, H., and Babcock, G. T. (2000) *Biochemistry 39*, 14371−14376.
25. Chu, H.-A., Gardner, M. T., Hillier, W., and Babcock, G. T. (2000) *Photosynth. Res. 66*, 57−63.
26. Noguchi, T., and Sugiura, M. (2001) *Biochemistry 40*, 1497−1502.
27. Hillier, W., and Babcock, G. T. (2001) *Biochemistry 40*, 1503−1509.
28. Chu, H.-A., Debus, R. J., and Babcock, G. T. (2001) *Biochemistry 40*, 2312−2316.
29. Kimura, Y., and Ono T.-A. (2001) *Biochemistry 40*, 14061−14068.
30. Chu, H.-A., Babcock, G. T., and Debus, R. J. (2001) in *Proceedings of the 12th International Congress on Photosynthesis*, S13-026, CSIRO Publishing, Collingwood, Australia.
31. Chu, H.-A., Hillier, W., Law, N. A., and Babcock, G. T. (2001) *Biochim. Biophys. Acta 1503*, 69−82.
32. Noguchi, T., and Sugiura, M. (2002) *Biochemistry 41*, 2322−2330.
33. Kimura, Y., Hasegawa, K., and Ono, T.-a. (2002) *Biochemistry 41*, 5844−5853.
34. Hasegawa, K., Kimura, Y., and Ono, T.-a. (2002) *Biochemistry 41*, 13839−13850.
35. Noguchi, T., and Sugiura, M. (2002) *Biochemistry 41*, 15706−15712.
36. Noguchi, T., and Sugiura, M. (2003) *Biochemistry 42*, 6035−6042.

37. Porter, R. D. (1988) *Methods Enzymol. 167*, 703−712.
38. Kashino, Y., Lauber, W. M., Carroll, J. A., Wang, Q., Whitmarsh, J., Satoh, K., and Pakrasi, H. B. (2002) *Biochemistry 41*, 8004−8012.
39. Nakamoto, K. (1986) *Infrared and Raman Spectra of Inorganic and Coordination Compounds*, pp 107−111, Wiley, New York.
40. Miyazawa, T., Shimanouchi, T., and Mizushima, S.-I. (1958) *J. Chem. Phys. 29*, 611−616.
41. Hasegawa, K., Ono, T.-a., and Noguchi, T. (2000) *J. Phys. Chem. B 104*, 4253−4265.
42. Tang, X.-S., Diner, B. A., Larsen, B. S., Gilchrist, M. L., Lorigan, G. A., and Britt, R. D. (1994) *Proc. Natl. Acad. Sci. U.S.A. 91*, 704−708.
43. Kitagawa, T. (1988) *Biological Applications of Raman Spectroscopy*, Vol. 3, pp 97−131, Wiley, New York.
44. Wells, A. V., Sage, J. T., Morikis, D., Champion, P. M., Chiu, M. L., and Sligar, S. G. (1991) *J. Am. Chem. Soc. 113*, 9655−9660.
45. Czarnecki, K., Chynwat, V., Erickson, J. P., Frank, H. A., and Bocian, D. F. (1997) *J. Am. Chem. Soc. 119*, 2594−2595.
46. Visser, H., Dubé, C. E., Armstrong, W. H., Sauer, K., and Yachandra, V. K. (2002) *J. Am. Chem. Soc. 124*, 11008−11017.
47. Cua, A., Stewart, D. H., Reifler, M. J., Brudvig, G. W., and Bocian, D. F. (2000) *J. Am. Chem. Soc. 122*, 2069−2077.
48. Cua, A., Vrettos, J. S., de Paula, J. C., Brudvig, G. W., and Bocian, D. F. (2003) *J. Biol. Inorg. Chem. 8*, 439−451.
49. Dave, B. C., and Czernuszewicz, R. S. (1998) *Inorg. Chim. Acta 281*, 25−35.

BI035420Q